Asymmetry in the bipolar signatures of flux transfer events

R. C. Fear[1], S. E. Milan[1], J. Raeder[2] and D. G. Sibeck[3]

23rd November 2010

Citation: Fear, R. C., S. E. Milan, J. Raeder and D. G. Sibeck (2010), Asymmetry in the bipolar signatures of flux transfer events, *J. Geophys. Res.*, **115**, A11217, doi:10.1029/2010JA015363.

[1]Department of Physics & Astronomy, University of Leicester, Leicester, LE1 7RH, United Kingdom.
[2]Department of Physics & Space Science Center, University of New Hampshire, 39 College Road, Durham, NH 03824-3525, USA
[3]Code 674, NASA/GSFC, Greenbelt, MD, 20771 USA

Correspondence to: r.fear@ion.le.ac.uk

Abstract

Several conceptual models have been proposed for the formation of flux transfer events (FTEs), including models based on reconnection at a single reconnection line (X-line) and at multiple X-lines. Two-dimensional magnetohydrodynamic models have previously been used to simulate both scenarios and have found a tendency for FTEs generated by single X-line reconnection to exhibit an asymmetry in the bipolar B_N signature that is the major in situ signature of FTE structures, with the leading peak being substantially smaller than the trailing peak. On the other hand, simulated FTEs generated by multiple X-line reconnection led to more symmetric signatures. We present a comparison of these simulation results with observations made at the Earth's magnetopause by the Cluster spacecraft, using a data set of 213 FTEs which were observed by all four spacecraft in 2002/3 at the high latitude magnetopause near local noon and at low latitudes on the flanks, and 36 FTEs which were observed by one or more Cluster spacecraft near the subsolar point in 2007 and 2008. A tendency is found for the B_N signatures to be asymmetric, but with the leading peak larger in amplitude than the trailing peak – opposite to the prediction made by the 2D single X-line simulations. This tendency is weaker in the subsolar FTEs. Therefore, the observations are not consistent with 2D MHD simulations of single X-line reconnection. The signatures observed near the subsolar point are more consistent with those predicted by 2D simulations of multiple X-line reconnection, although the multiple X-line simulation studies did not report any net asymmetry. We propose that the observed asymmetry can be explained by a compression of magnetic flux ahead of the propagating FTE structure, and a rarefaction behind it. The weaker tendency nearer the subsolar point is consistent with a weaker compression and rarefaction due to lower FTE velocities.

1 Introduction

Flux transfer events, or FTEs, are bursts of magnetic reconnection at the dayside magnetopause which cause characteristic in situ and ionospheric signatures (*Russell and Elphic*, 1978, 1979; *Elphic et al.*, 1990). At the magnetopause, FTEs are characterized by a bipolar signature in the component of the magnetic field normal to the magnetopause (B_N). Whilst *Russell and Elphic* (1978) interpreted the observed signatures in terms of a flux tube formed at a small reconnection site (of order 1 R_E in extent), others have proposed alternative interpretations. *Southwood et al.* (1988) and *Scholer* (1988) suggested that FTEs could be "bulges" formed by bursty reconnection at a single X-line of arbitrary length. Ahead of the X-line, heated plasma causes an increase in the thermal pressure, causing the boundary layer (and hence magnetic field lines) to bulge outwards. *Lee and Fu* (1985) interpreted the signatures as flux ropes which were formed between multiple X-lines, and *Sibeck* (1990, 1992) developed a model which did not require reconnection at all, but was based on magnetopause indentations caused by pressure pulses. In this paper, we aim to compare magnetopause observations of FTEs with characteristics of FTEs observed in simulations to explore the differences between some of the models.

These models have been reviewed by *Scholer* (1995), *Lockwood and Hapgood* (1998) and *Fear et al.* (2008). *Lockwood and Hapgood* (1998) examined one FTE observed by two of the AMPTE spacecraft and concluded that its plasma signatures and motion were not consistent with the *Russell and Elphic* or *Lee and Fu* models, but were consistent with the *Southwood et al./Scholer* single X-line model. Due to the long time between the FTE observation and the subsequent entry of the spacecraft into the magnetosheath, *Lockwood and Hapgood* could not exclude the pressure pulse model as an explanation if reconnection was occurring simultaneously. Ionospheric observations have shown that FTEs may extend across several hours of local time (*Milan et al.*, 2000), which is more likely to be consistent with the *Lee and Fu* or *Southwood et al./Scholer* models. Multi-spacecraft observations have also shown that FTEs can occur with long azimuthal extents (*Fear et al.*, 2008), but small-scale, patchy events are observed too (*Fear et al.*, 2010), indicating that individual events can contribute varying amounts to the global reconnection-driven ionospheric convection process.

In a series of papers, *Ding et al.* (1991) and *Ku and Sibeck* (1997, 1998a,b, 2000) carried out two dimensional MHD simulations of FTEs in which they compared the signatures observed by the passage of FTEs formed by the single and multiple X-line models. *Ding et al.* (1991) simulated both single and multiple X-line reconnection, *Ku and Sibeck* (1997, 1998a,b) simulated the single X-line scenario and *Ku and Sibeck* (2000) simulated multiple X-lines. All of the single X-line studies found that the B_N signatures of the simulated FTEs were highly asymmetric, with the first (leading) peak of the bipolar signature being much weaker than the second (trailing) peak. This occurred under a range of reconnection scenarios, which differed between studies: *Ding et al.* (1991) modeled a "pulse", where the resistivity at the X-line was ramped up and then decayed; the resistivity in *Ku and Sibeck* (1997, 1998a) was increased from zero and then remained steady and in *Ku and Sibeck* (1998b) it was increased and then abruptly switched off. Whilst the asymmetry has been reproduced in all of these studies, it is possible that this effect is due to the two dimensional nature of the simulations (*Lockwood and Hapgood*, 1998).

Ding et al. (1991) also noted that as B_{sphere}/B_{sheath} was increased, the asymmetry in the B_N signatures increased and the magnitude of the B_N signatures decreased. In the *Ku and Sibeck* single X-line simulations, the signatures became larger in magnitude and less asymmetric with time as they propagated away from the X-line.

Furthermore, magnetospheric signatures are sometimes absent in 2D MHD single X-line simulations. If the ratio of the magnetospheric to magnetosheath magnetic field strength B_{sphere}/B_{sheath} is greater than about 1.5 (*Scholer*, 1989) or 1.7 (*Ding et al.*, 1991), then the simulated 'bulge' of reconnected flux extends out mainly onto the magnetosheath side of the magnetopause, and therefore identifiable magnetospheric FTE signatures are absent. All of the *Ku and Sibeck* single X-line simulations used a ratio of 2.0, and classical magnetospheric signatures were absent.

Ding et al. (1991) and *Ku and Sibeck* (2000) simulated multiple X-line reconnection, using two X-lines. In these simulations, "bulges" identical to those formed in the single X-line scenario were produced outside the two X-lines. In addition, magnetic islands (2D slices of flux ropes) were formed between the X-lines. (Note that Figure 1b of *Lee and Fu* (1985) shows reconnected magnetic field lines outside the outermost X-lines which do not form part of the flux rope – in fact, most of the open flux which traces down to the ionosphere does not map through the flux rope (*Fear et al.*, 2008).) The "bulges" produced the same signatures as in the single X-line simulations, but the islands (flux ropes) produced more symmetric bipolar B_N signatures. Therefore the multiple X-line simulations produced both asymmetric and symmetric signatures, where the relative occurrence rate will more generally depend upon the number of X-lines. The flux rope signatures were observed in both the magnetosheath and the magnetosphere for B_{sphere}/B_{sheath} ratios up to 2.6, and the magnitude of the B_N signatures produced by the flux ropes decreased as B_{sphere}/B_{sheath} was increased (*Ding et al.*, 1991). The imposed reconnection rate also differed between the two studies: *Ding et al.* (1991) used resistivity time series at two X-lines which were constant in time and equal at both X-lines (in which case, the only force acting on the flux rope is that exerted by the magnetosheath flow). *Ku and Sibeck* (2000) used resistivities which ramped up to an asymptote and they examined both equal and unequal reconnection rates at the two X-lines and the effect of a magnetosheath flow.

Therefore there are two predictions from the 2D simulation studies which we seek to test in this paper. First, all of these studies predict an asymmetric B_N signature with a dominant trailing peak amplitude for structures formed by single X-line reconnection, and symmetric B_N signatures for flux ropes formed by multiple X-lines. Second, if the ratio B_{sphere}/B_{sheath} is between about 1.7 and 2.6, then the simulations predict that magnetospheric signatures of structures formed by single X-line reconnection should be difficult to detect.

Only one study has discussed satellite observations of the asymmetry in flux transfer event B_N signatures in a quantitative manner. *Sanny et al.* (1998) examined FTEs observed by the AMPTE CCE spacecraft and defined the amplitudes of the leading and trailing peaks to be α and β respectively. None of the 110 FTEs they examined exhibited a significantly larger amplitude in the leading peak than in the trailing peak; 79 out of 110 events were symmetric or nearly symmetric ($\alpha \geq 0.75\beta$), and the remaining 31 events were characterized by asymmetric B_N signatures in which the trailing peak was significantly larger in amplitude than the leading peak ($\alpha < 0.75\beta$). In the context of the *Ding et al.* and *Ku and Sibeck* simulations, this might appear to be more consistent with FTEs being formed by multiple X-line reconnection. However, *Sanny et al.* (1998) noticed that most of the asymmetric events were observed near the magnetic equator; they concluded that this was consistent with the formation of asymmetric FTEs at low latitudes by single X-line reconnection, which then evolved into more symmetric events as they propagated to higher latitudes as simulated by *Ku and Sibeck*. *Sanny et al.* (1998) also compared the occurrence of magnetospheric and magnetosheath FTE signatures with the ratio B_{sphere}/B_{sheath}, measured at the nearest magnetopause crossing. The magnetosheath signatures were all observed when $B_{sphere}/B_{sheath} \leq 2.2$, whereas magnetospheric signatures were observed up to $B_{sphere}/B_{sheath} = 7$ but with a sharp decrease above $B_{sphere}/B_{sheath} = 3$. However the smaller "detectability criterion" used by *Sanny et al.* increased the B_{sphere}/B_{sheath} cutoffs predicted by *Ding et al.*, and so *Sanny et al.* concluded that their B_{sphere}/B_{sheath} observations could not be interpreted as favoring one model over the other.

In the following section, we examine the asymmetry observed in flux transfer events detected by Cluster. First we discuss the statistics of 213 FTEs which were observed between November 2002 and June 2003, when the orbit of the Cluster spacecraft crossed the magnetopause at high latitudes near noon (local time), and at lower latitudes on the flanks. Due to the difference in the orbits of AMPTE and Cluster, these observations occur further from the subsolar point than those reported by *Sanny et al.* (1998). Then we discuss a further 36 FTEs which were observed in March 2007 and March/April 2008; in these months, the Cluster spacecraft crossed the magnetopause within 3 R_E of the subsolar point, making the latter group of observations directly comparable with the results reported by *Sanny et al.* (1998). Contrary to the observations of *Sanny et al.*, we observe a tendency for the bipolar signature to be asymmetric with a leading peak that is larger in amplitude than the trailing peak, which is opposite to the simulation predictions. This tendency is weaker (but still present) near the subsolar point. Finally, we discuss our results and conclude.

2 Cluster observations

The locations of the flux transfer event signatures used in this study are shown in Figure 1. In the early phases of the Cluster mission, the spacecraft crossed the dayside magnetopause at high latitudes near local noon, and at lower latitudes on the flanks. The outer ring of FTE signatures in Figure 1 [all of which were observed in the range 6 $R_E < (Y_{GSM}^2 + Z_{GSM}^2)^{\frac{1}{2}} <$ 19 R_E] were observed by the Cluster spacecraft between November 2002 and June 2003, and were used in a statistical study by *Fear et al.* (2005, 2007). These high latitude and flank signatures will be discussed in Section 2.1.

More recently, the orbit of the Cluster spacecraft has evolved such that it crosses the dayside magnetopause at lower latitudes during the outbound leg of the orbit. The signatures in Figure 1 observed at $(Y_{GSM}^2 + Z_{GSM}^2)^{\frac{1}{2}} < 3$ R_E [within the dotted circle] were observed by Cluster in March 2007 and March/April 2008. These subsolar events will be discussed in Section 2.2.

2.1 High latitude and flank observations

For the analysis of high latitude and flank FTEs, we use the catalogue of flux transfer events observed by Cluster and reported by *Fear et al.* (2005, 2007). As discussed by *Fear et al.* (2005), the FTEs were identified in the magnetic field data provided by the Flux Gate Magnetometer (FGM) instrument (*Balogh et al.*, 2001) by plotting the data at 4 s resolution in a boundary normal coordinate frame derived from the *Roelof and Sibeck* (1993) model. (The data were also examined simultaneously in a coordinate frame derived from minimum variance analysis on the nearest magnetopause crossing.) Events were identified manually with the criteria of a bipolar variation in B_N that was clear in relation to the background variation of the magnetic field, and a variation (enhancement or decrease) in $|\mathbf{B}|$. No threshold was set for the B_N variation. The B_N signature was not required to be symmetrical, but since *Fear et al.* (2005) wished to exclude non-FTE events from their catalogue, a 'clear' bipolar B_N signature was required at at least one of the four spacecraft. This resulted in a list of 446 FTEs which were observed by at least one spacecraft. *Fear et al.* (2007) then shortlisted the FTEs which exhibited an identifiable bipolar signature at all four spacecraft (213 events). In this subsection, we consider only those 213 FTEs. In all subsequent analysis we use higher resolution data (5 Hz) than that used to identify the FTEs, and we use a more recent magnetopause model developed by *Shue et al.* (1998). We calculate the boundary normal coordinate system separately for each spacecraft, and we consider each B_N trace separately, i.e. as 852 independent FTEs. This has the advantage over use of single-spacecraft data that we consider weaker bipolar signatures which might not have been spotted by themselves, but which are identifiable once a clearer signature on another spacecraft has been located.

Each B_N trace was analyzed using the following procedure. First, any offset in the B_N component was removed by subtracting the mean value of B_N, evaluated over a 20 minute interval around the FTE, from the time series. Then, a low pass filter with a cutoff period of 20 s was applied to remove any short-term variations – typically magnetosheath noise, but also some FTE substructure. (Neither *Sanny et al.* (1998) nor the authors of the 2D MHD simulations filtered their data, but *Sanny et al.* used lower cadence magnetic field data (6 s) than in the present study, and the simulated signatures shown by *Ding et al.* (1991) and in the *Ku and Sibeck* papers were smooth without the need for filtering.) All signatures were then examined by plotting both the filtered and unfiltered data, to ensure that the main bipolar signature was not filtered out. An example is shown in Figure 2, which shows the B_N traces observed by all four spacecraft for an FTE which was observed on the 10th November 2002 at 11:43 UT, and which illustrates the fact that the same FTE can give rise to differing degrees of asymmetry if observed at different distances from the magnetopause. The peak amplitudes of the filtered B_N traces were identified for the leading and trailing peaks, along with the times at which they occurred (dashed guidelines). Then the widths of the peaks were determined by measuring the time the filtered trace exceeded three threshold values: 25%, 50% and 75% of the peak amplitude. Finally, the area of the peak was calculated by integrating the filtered trace in the range of time in which it exceeded each threshold value. The widths and areas of the trace when it exceeded 75%, 50% and 25% of the peak amplitudes are indicated in Figure 2 by blue shading; blue & red; and blue, red & green shading respectively. The peak amplitudes, widths and areas (evaluated at 25% of the peak amplitude) of the example B_N traces in Figure 2 are given in Table 1.

The asymmetry of each FTE trace is plotted in Figure 3, which shows the amplitude of the leading peak of each trace against the amplitude of the trailing peak, and shows the number and percentage of B_N traces where the amplitude of the leading peak is greater than, less than, and equal to the amplitude of the trailing peak. In two thirds of all cases (566 traces), the amplitude of the leading peak was greater than the amplitude of the trailing peak, contrary to the sense of the asymmetry in the single X-line simulations reported by *Ding et al.* (1991) and *Ku and Sibeck* (1997, 1998a,b), and also contrary to the observations of *Sanny et al.* (1998). The observed tendency for an asymmetric signature with a larger amplitude leading peak is also different from the symmetric signatures resulting from multiple X-line simulations reported by *Ding et al.* (1991) and *Ku and Sibeck* (2000).

The asymmetries of the peak widths and areas are shown in Figure 4; each panel follows the same format as Figure 3, and shows the full widths at quarter, half and three-quarter maximum and the peak areas (the shaded areas in Figure 2). It is evident that there is a tendency for the trailing peak to last longer than the leading peak, whichever width measurement is used, and that trend is clearest when the width is measured at one quarter of the peak amplitude. We interpret the trend for a larger amplitude leading peak followed by a weaker, but longer-duration trailing peak to be due to a compression of the magnetic flux (both the unreconnected flux which drapes around the FTE and the reconnected flux which forms the 'core' of the structure) on the leading edge of the FTE due to the motion of the structure, and a rarefaction on the trailing edge.

There is not such a clear trend when the areas of each peak are compared, and there is plenty of scatter. Whilst the area of the leading peak predominates when measured between the points where the trace exceeds the three-quarter maximum threshold, the proportion of events with a larger leading peak area diminishes as the threshold decreases – i.e. as the proportion of the peak that is included in the integration increases. (Only 52% of events have a larger leading peak area when the area is measured between the points where the trace exceeds the one-quarter maximum threshold.) We interpret this as being due to the fact that for most possible paths a spacecraft may take through an idealized FTE (formed by any of the above-mentioned models), the total amount of flux that is observed directed outwards in the positive B_N peak is matched by the flux that is observed directed inwards in the negative peak. The exceptions are in the single X-line model where a spacecraft is on open magnetic field lines before observing the FTE, and passes close to the center of the event (i.e. a spacecraft which is very close to the magnetopause before the passage of the FTE), and in the *Russell and Elphic* flux tube model where the spacecraft passes close to the 'hole' in the magnetopause. In both cases the spacecraft will observe a small imbalance in the net flux. The scatter in Figure 4b indicates that whilst this may be true on average, there is a great deal of irregularity in individual cases.

In summary, the trend in the high latitude and flank events observed by Cluster is for the leading peak to be larger than the trailing peak, but for the trailing peak to have a longer duration. The areas under the B_N traces are on average nearly equal, indicating equal quantities of flux being deflected outwards and inwards around (and within) the FTE on average. We could not find any deviation from these trends on subsetting the data by location (magnetosphere/magnetosheath), B_N polarity, interplanetary magnetic field B_Z component or magnetic local time.

Ding et al. (1991) reported that in their simulations, magnetospheric FTEs were only observable if the ratio B_{sphere}/B_{sheath} was less than 1.7, but magnetospheric FTEs are a common occurrence, both in general and in our dataset. If spacecraft straddle the magnetopause as an FTE is observed, we can directly measure this ratio immediately before or after the passage of the FTE. Out of the 213 shortlisted FTEs, only nine FTEs (on five different orbits) were observed by at least one spacecraft located in the magnetosheath and at least one situated in the magnetosphere-proper. (A further 14 FTEs were observed when the spacecraft straddled the magnetopause, but the magnetospheric spacecraft were located in a boundary layer containing some magnetosheath-energy plasma, in which the magnetic field would be expected to be suppressed relative to that in the magnetosphere-proper.) In all nine cases the ratio B_{sphere}/B_{sheath}, measured outside the FTE, was less than 1.6, and was therefore within the domain in which magnetospheric FTEs would be observed in both the *Ding et al.* (1991) single and multiple X-line simulations. Therefore in these cases, the ratio B_{sphere}/B_{sheath} at the time of observation of magnetospheric FTE signatures cannot be used to discriminate between the Cluster observations and each of the simulated scenarios.

2.2 Subsolar observations

The peak amplitude asymmetry observations reported in the previous subsection differ from those reported by *Sanny et al.* (1998) and from the predictions of both the single and multiple X-line simulations. To test whether this is due to the different locations of the FTE observations (and hence assumed distance from a subsolar reconnection site), we examined the Cluster magnetopause crossings from March 2007 and March/April 2008. FTE signatures were identified using the same criteria as *Fear et al.* (2005). For consistency with Section 2.1, the FTE signatures were first identified in the 4 s resolution FGM data, and the subsequent analysis used 5 Hz data. In order to compare closely with *Sanny et al.*, only FTE signatures observed in the region where $(Y^2_{GSM} + Z^2_{GSM})^{\frac{1}{2}} < 3\ R_E$ were included. From a total of 23 magnetopause crossings which satisfied the subsolar location criterion, 36 independent flux transfer events were observed. Since only 12 events were observed by all four spacecraft, we did not discard those events only observed by a subset of the spacecraft; this may result in a bias towards clearer, more conventional signatures. Treating the FTE signatures observed at multiple spacecraft independently resulted in 85 bipolar B_N traces (comparable to the 110 FTEs in the survey of *Sanny et al.* (1998)), to which the analysis described in Section 2.1 was applied.

A comparison of the leading and trailing peak amplitudes is shown in Figure 5. Although the statistics are poorer than in Figure 3, it can be seen that the trend for larger amplitude leading peaks that was observed in Section 2.1 is not so clearly present: the numbers of cases where the leading and trailing peaks dominate are approximately equal. In the top three rows of Table 2 we have subdivided the high latitude/flank events from Section 2.1, the subsolar events from this subsection and the events reported by *Sanny et al.* (1998) into a classification based on that used by *Sanny et al.*. In their Table 1, *Sanny et al.* reported no events where the leading peak was significantly larger than the trailing peak, whereas some such events are present in our subsolar dataset (Figure 5). *Sanny et al.* (1998) defined events to be 'symmetric or nearly symmetric' if $\alpha > 0.75\beta$; we therefore define our FTE signatures to be 'symmetric or nearly symmetric' if $1.25\beta > \alpha > 0.75\beta$. Most of *Sanny et al.*'s events were observed within 3 R_E of the subsolar point, which is equivalent to our subsolar observations. In the division used in Table 2, a distinction becomes clear: 41% of the Cluster subsolar B_N traces exhibited a significantly larger leading peak amplitudes. Only 26% of the Cluster subsolar signatures were symmetric or nearly symmetric (compared with 72% of *Sanny et al.*'s events), but the proportion classified as asymmetric with a larger trailing peak amplitude (33%) was similar to that observed by *Sanny et al.* (28%). Therefore, as in Section 2.1, the Cluster observations near the subsolar point are inconsistent with the single X-line simulations carried out by *Ding et al.* (1991) and *Ku and Sibeck* (1997, 1998a,b). Although there is still a bias observed towards events with a larger leading peak amplitude, this is weaker than at high latitudes: the proportions of the signatures in the 'large leading peak amplitude' and 'symmetric or nearly symmetric' categories in the current study are both lower in the subsolar region than at higher latitudes and on the flank, and the proportion of events in the 'large trailing peak amplitude' category is slightly higher in the subsolar region (Table 2). Therefore, the subsolar observations are still not quite consistent with the predictions of the multiple X-line simulations of *Ding et al.* (1991) and *Ku and Sibeck* (2000), but as the trend for large leading peak amplitudes is weaker than that observed further from the subsolar point, the discrepancy between the multiple X-line simulations and the observations is less significant than in Section 2.1.

The asymmetry in the widths and areas of the peaks of the subsolar signatures observed by Cluster is shown in Figure 6. Contrary to the high latitude/flank observations, there is a weak tendency for the width of the leading peak to be longer than that of the trailing peak (Figure 6a). Combined with the larger proportion of signatures with greater leading peak amplitudes (Figure 5), this results in tendency for the area under the leading peak to be larger than the area under the trailing peak (Figure 6b).

3 Discussion

In this section, we compare the observations reported above with the 2D MHD simulations of flux transfer events undertaken by *Ding et al.* (1991) and *Ku and Sibeck* (1997, 1998a,b, 2000) and with the only previously reported statistical observational study of B_N asymmetry (*Sanny et al.*, 1998). The simulations predicted that a key difference between the observed signatures of flux transfer events formed by the bursty single X-line model (*Southwood et al.*, 1988; *Scholer*, 1988) and those formed by the multiple X-line model (*Lee and Fu*, 1985) would be that multiple X-line FTEs would produce a symmetric bipolar B_N signature, whereas single X-line events (including such events formed at the outermost pair of X-lines in the multiple X-line model) would produce asymmetric signatures with the trailing peak significantly larger in amplitude than the leading peak. In the preceding section, we have shown that Cluster observed a weak tendency for a larger leading peak amplitude in the subsolar region, and a much clearer tendency for the same asymmetry further from the subsolar point. On the face of it, these observations do not appear to match the simulation predictions for either single or multiple X-line reconnection, but this point will be discussed further below. Our observations also contradict those reported by *Sanny et al.* (1998), which we will discuss in Section 3.3. In order to determine the validity of the comparison between the Cluster observations and the 2D MHD predictions, we will first discuss the size of the simulation domain used by *Ding et al.* and *Ku and Sibeck*.

3.1 Extent of simulation domain

The *Ku and Sibeck* (1997, 1998a,b, 2000) simulation domains were dimensionless, being normalized to a scale length ℓ which was defined relative to the magnetopause boundary thickness. *Ku and Sibeck* (1997) defined the thickness of the magnetopause layer on the magnetospheric side of the boundary as h, the thickness of the magnetopause layer on the magnetosheath side as hB_{sheath}/B_{sphere}, and $\ell = h/2$. (Therefore if, as in all of the *Ku and Sibeck* simulations, $B_{sheath}/B_{sphere} = 0.5$, then the total magnetopause thickness is 3ℓ.) The *Ku and Sibeck* simulation domains extended to between 170ℓ and 230ℓ from the reconnection site, in the direction tangential to the magnetopause. If we take a typical value of ℓ=150 km (*Ku and Sibeck*, 1997), then the simulation domains were 4 to 5 R_E long along the magnetopause, and the magnetopause thickness is 450 km (which is of the same order as magnetopause thicknesses deduced from previous multi-spacecraft measurements (*Berchem and Russell*, 1982; *Haaland et al.*, 2004)). The simulation domain used by *Ding et al.* (1991) was smaller; scale lengths were normalized to the parameter a, which was the half-thickness of the magnetopause current sheet, and the simulation domain was extended to $20a$ from the reconnection site. A magnetopause current sheet thickness of 450 km is equivalent to a simulation domain that is 4500 km long along the magnetopause.

All of the FTEs reported in Section 2.2, and most of those reported by *Sanny et al.* (1998), were observed within 3 R_E of the subsolar point. It is therefore likely that they were observed within $\sim$3 R_E of their reconnection site. Consequently, the tangential extents of the *Ku and Sibeck* simulation domains are roughly equivalent to the latitudinal range of both the *Sanny et al.* (1998) observations and those presented in Section 2.2, and the simulations can be compared directly with the near-subsolar observations. On the other hand, since the orbit of Cluster in 2002/3 did not sample the subsolar magnetopause, any FTEs in Section 2.1 which were formed near the subsolar point were observed at a later stage of their evolution than was simulated by *Ding et al.* or *Ku and Sibeck*.

3.2 Comparison with simulations and physical interpretation

Just under half (46%) of the 85 B_N traces examined in Section 2.2 had trailing peaks with larger amplitudes than the leading peaks. In Section 2.2 (Table 2), the events were also divided into the categories used by *Sanny et al.* (1998), and only 33% of the traces were classified as 'large trailing peak amplitude' events, compared with 26% which were broadly symmetric ($1.25\beta > \alpha > 0.75\beta$) and 41% which had a leading peak amplitudes which were significantly larger than the trailing peaks. Despite the fact that the events reported in Section 2.2 are the most directly comparable in location with the MHD simulations, the single X-line simulations are clearly very different from the Cluster observations. Therefore, we cannot confirm the conclusions of *Sanny et al.* (1998) that the observed asymmetry is consistent with the single X-line modeling of *Ding et al.* (1991) and *Ku and Sibeck* (1997, 1998a,b).

Neither *Ding et al.* (1991) nor *Ku and Sibeck* (2000) reported the asymmetry observed in this study to be present in the B_N signatures caused by flux ropes from multiple X-line reconnection, so the subsolar Cluster observations do not quite match the multiple X-line predictions either. However, the asymmetry in the subsolar Cluster signatures only becomes clear when we use the categorization used by *Sanny et al.* (1998), and both *Ding et al.* (1991) and *Ku and Sibeck* (1997, 1998a,b, 2000) qualitatively described the B_N signatures in their simulations, rather than systematically measuring the ratio of the peak amplitudes. Therefore it is possible that the observed trend for asymmetry near the subsolar point is weak enough for it not to stand out in the MHD simulation runs. Although we are not aware of any recent 3D attempts to simulate FTE signatures based on single X-line reconnection, and a comparison with such a simulation would be interesting, a variety of global MHD and hybrid models now exist. In these models, flux transfer events are interpreted as being formed by a variety of mechanisms including multiple X-line reconnection (e.g. *Raeder*, 2006; *Omidi and Sibeck*, 2007; *Sibeck et al.*, 2008), global separator reconnection (*Fedder et al.*, 2002), and flow vortices where separator reconnection is an effect rather than a cause of the FTE structures (*Dorelli and Bhattacharjee*, 2009). The asymmetry in FTE B_N signatures observed by Cluster, both near the subsolar point and nearer the terminator, provides an additional test for such models.

Our physical interpretation for the predominance of a larger leading peak amplitude and a longer, but weaker, trailing peak is that it is consistent with a compression of the magnetic flux on the leading edge of the FTE structure and a rarefaction behind. This effect is seen more clearly further from the subsolar point (Section 2.1). In this region, one would expect FTE structures to have higher velocities due to the larger magnetosheath flow speed (which, along with the magnetic tension in the reconnected magnetic field lines, influences the speed of an FTE structure (*Cowley and Owen*, 1989)); the increased strength of the observed trends at distances further from the subsolar point is consistent with an enhanced compression and rarefaction due to larger FTE speeds. However, the weak tendency in the subsolar region for trailing peaks which are shorter in duration than the leading peaks (which is opposite to the trend observed further from the subsolar point) does not fit with this simple picture. Since the *Ding et al.* (1991) and *Ku and Sibeck* (2000) multiple X-line simulations both simulated a limited region around the X-line, one might expect the velocities of the simulated structures to be low compared with those of real events observed far from the subsolar point, which might explain the lack of a strong compression/rarefaction effect in the multiple X-line simulations.

Finally in this section, we note that a second key prediction made by *Ding et al.* (1991) was that according to their simulations of single X-line reconnection, magnetospheric FTEs should not be observed unless the ratio B_{sphere}/B_{sheath} was less than 1.7. Magnetospheric signatures could be observed in their multiple X-line simulations if B_{sphere}/B_{sheath} was up to 2.6. Only nine of the FTEs analyzed in Section 2.1 occurred when the Cluster tetrahedron straddled the magnetopause and observed both the magnetosheath and the magnetosphere-proper, and in all of these cases B_{sphere}/B_{sheath} was less than 1.6. Therefore the ratio B_{sphere}/B_{sheath} in this handful of events was always in the range in which discernible magnetospheric FTE signatures were observed in both the *Ding et al.* (1991) single and multiple X-line simulations.

3.3 Discrepancy with *Sanny et al.* (1998)

Sanny et al. (1998) investigated the asymmetry in FTE B_N signatures observed within 5 R_E of the subsolar point by AMPTE CCE. None of their reported events exhibited a larger amplitude in the leading peak than in the trailing peak; the majority of events (72%) were classified as symmetric or nearly symmetric, and the remainder were asymmetric with a larger trailing peak amplitude. 26% of our subsolar FTE traces can be regarded as nearly symmetric ($1.25\beta \geq \alpha \geq 0.75\beta$), 33% as strongly asymmetric with a dominant trailing peak ($\alpha < 0.75\beta$), and 41% as strongly asymmetric with a dominant leading peak ($\alpha > 1.25\beta$). Comparing our subsolar observations with those of *Sanny et al.* (1998), it is clear that the reason for the discrepancy between their observations and ours is not due to the distance from the X-line, since the two sets of observations covered similar regions of the magnetopause. There are some slight differences in the procedures used in the present study and by *Sanny et al.* (1998). *Sanny et al.* identified their events by examining the magnetic field data in the GSE coordinate system, and subsequently checked their events by carrying out minimum variance analysis on the nearest magnetopause crossing and plotting the data in the resulting boundary normal coordinate frame. In this study, the events were identified using magnetometer data plotted in a boundary normal coordinate frame derived from a magnetopause model. (*Fear et al.* (2005) used the *Roelof and Sibeck* (1993) model and examined simultaneously the data in a minimum variance frame. In order to identify the low latitude events used in Section 2.2, we used a more recent magnetopause model developed by *Shue et al.* (1998).) However, the use of GSE coordinates by *Sanny et al.* for initial event selection should not lead to a systematic bias in asymmetry. *Sanny et al.* used 6 s resolution magnetic field data – similar to the 4 s resolution data used for event selection in the present study. Finally, *Sanny et al.* considered only events with a duration of at least 1 minute, and with a peak-to-peak B_N amplitude of at least 5 nT. From the traces used in Section 2.2, 64 match these two selection criteria. This subset exhibits a similar breakdown of asymmetries (shown in the bottom line of Table 2) to that observed in the full set of FTEs in Section 2.2. Therefore, we cannot provide an explanation for why we observe more asymmetric subsolar events (with a dominant leading peak) than *Sanny et al.* (1998). Indeed, it is perhaps surprising that in a survey of 110 FTEs, *Sanny et al.* did not find a single FTE which exhibited a significantly larger amplitude in its leading peak. We do note, though, that as the apogee of AMPTE CCE was only 8.8 R_E, the FTE signatures observed by AMPTE CCE occurred when the magnetopause was either significantly compressed, eroded, or both. Consequently, the observations reported by *Sanny et al.* (1998) do not correspond to intervals of typical solar wind conditions.

4 Conclusions

We have presented an analysis of the asymmetry in the bipolar B_N signatures of 213 flux transfer events observed by Cluster at high latitudes and on the magnetopause flank in 2002/3, and 36 FTEs observed by Cluster in the subsolar region in 2007 and 2008. We have compared our results with predictions based on 2D MHD simulations by *Ding et al.* (1991) and *Ku and Sibeck* (1997, 1998a,b, 2000). The simulations predicted mostly symmetric B_N signatures for FTEs formed by multiple X-line reconnection, and asymmetric signatures (with a dominant trailing peak) for FTEs formed by single X-line reconnection. In the subsolar region, which is equivalent in location of the MHD simulation domains, 41% of the FTE traces observed by Cluster were asymmetric with a larger leading peak amplitude; 26% were broadly symmetric and only 33% were asymmetric in the sense predicted by the single X-line simulations. Therefore the Cluster subsolar observations are not consistent with the single X-line MHD predictions, and the observed asymmetry also differs from previous observations reported by *Sanny et al.* (1998). The observations are also not quite consistent with the multiple X-line simulations, as these simulations predicted symmetric events rather than the signatures with larger leading peak amplitudes that were observed by Cluster. However, since the observed trend for asymmetry is comparatively weak near the subsolar point, it is possible that it is too weak to stand out in the *Ding et al.* (1991) and *Ku and Sibeck* (2000) simulations.

The same sense of asymmetry was generally observed by Cluster further from the subsolar point, but the proportion of signatures with a larger leading peak amplitude was even higher and the proportion with a larger trailing peak amplitude was lower. At these distances, the trailing peaks tended to have a longer duration than the duration of the leading peaks. The asymmetry observed by Cluster is consistent with a compression of the magnetic field ahead of the moving FTE structure, and a rarefaction behind it.

Several global MHD and hybrid models now exist, in which flux transfer events are interpreted as being formed by a variety of different mechanisms. The asymmetry observed by Cluster in FTE signatures both near the subsolar point and nearer the terminator provide an additional test for these models.

Acknowledgments

This study was carried out as part of the International Space Science Institute international team on “Advances in understanding of the structure and dynamics of magnetic flux transfer at the Earth’s magnetopause”; we gratefully acknowledge ISSI’s support and discussions with other team members (A. Marchaudon, K. A. McWilliams, C. J. Owen, Y. Wang and J. A. Wild). We thank E. A. Lucek and the Cluster Active Archive (http://caa.estec.esa.int/) for data from the Cluster FGM instrument. Work at the University of Leicester was supported by STFC grant PP/E000983/1. We also thank the referees for their constructive suggestions.

References

Balogh, A., C. M. Carr, M. H. Acuña, T. J. Beek, M. W. Dunlop, P. Brown, K.-H. Fornaçon, E. Georgescu, K. H. Glassmeier, J. Harris, G. Musmann, T. Oddy, and K. Schwingenschuh (2001), The Cluster Magnetic Field Investigation: overview of in-flight performance and initial results, *Ann. Geophys.*, *19*, 1207–1217.

Berchem, J., and C. T. Russell (1982), The thickness of the magnetopause current layer: ISEE 1 and 2 observations, *J. Geophys. Res.*, *87*(A4), 2108–2114, doi:10.1029/JA087iA04p02108.

Cowley, S. W. H., and C. J. Owen (1989), A simple illustrative model of open flux tube motion over the dayside magnetopause, *Planet. Space Sci.*, *37*, 1461–1475, doi:10.1016/0032-0633(89)90116-5.

Ding, D. Q., L. C. Lee, and Z. W. Ma (1991), Different FTE signatures generated by the bursty single X-Line reconnection and the multiple X-Line reconnection at the dayside magnetopause, *J. Geophys. Res.*, *96*(A1), 57–66, doi:10.1029/90JA01989.

Dorelli, J. C., and A. Bhattacharjee (2009), On the generation and topology of flux transfer events, *J. Geophys. Res.*, *114*, A06213, doi:10.1029/2008JA013410.

Elphic, R. C., M. Lockwood, S. W. H. Cowley, and P. E. Sandholt (1990), Flux transfer events at the magnetopause and in the ionosphere, *Geophys. Res. Lett.*, *17*(12), 2241–2244.

Fear, R. C., A. N. Fazakerley, C. J. Owen, and E. A. Lucek (2005), A survey of flux transfer events observed by Cluster during strongly northward IMF, *Geophys. Res. Lett.*, *32*(18), L18105, doi:10.1029/2005GL023811.

Fear, R. C., S. E. Milan, A. N. Fazakerley, C. J. Owen, T. Asikainen, M. G. G. T. Taylor, E. A. Lucek, H. Rème, I. Dandouras, and P. W. Daly (2007), Motion of flux transfer events: a test of the Cooling model, *Ann. Geophys.*, *25*, 1669–1690.

Fear, R. C., S. E. Milan, A. N. Fazakerley, E. A. Lucek, S. W. H. Cowley, and I. Dandouras (2008), The azimuthal extent of three flux transfer events, *Ann. Geophys.*, *26*, 2353–2369.

Fear, R. C., S. E. Milan, E. A. Lucek, S. W. H. Cowley, and A. N. Fazakerley (2010), Mixed azimuthal scales of flux transfer events, in *The Cluster Active Archive - Studying the Earth's Space Plasma Environment*, edited by H. Laakso, M. Taylor, and C. P. Escoubet, Astrophys. Space Sci. Proc., pp. 389–398, Springer Netherlands, Dordrecht, doi:10.1007/978-90-481-3499-1_27.

Fedder, J. A., S. P. Slinker, J. G. Lyon, and C. T. Russell (2002), Flux transfer events in global numerical simulations of the magnetosphere, *J. Geophys. Res.*, *107*(A5), doi:10.1029/2001JA000025.

Haaland, S. E., M. W. Dunlop, B. U. O. Sonnerup, A. Balogh, E. Georgescu, H. Hasegawa, B. Klecker, G. Paschmann, P. Puhl-Quinn, H. Rème, H. Vaith, and A. Vaivads (2004), Four-spacecraft determination of magnetopause orientation, motion and thickness: comparison with results from single-spacecraft methods, *Ann. Geophys.*, *22*, 1347–1365.

Ku, H. C., and D. G. Sibeck (1997), Internal structure of flux transfer events produced by the onset of merging at a single X line, *J. Geophys. Res.*, *102*(A2), 2243–2260, doi:10.1029/96JA03162.

Ku, H. C., and D. G. Sibeck (1998a), The effect of magnetosheath plasma flow on flux transfer events produced by the onset of merging at a single X line, *J. Geophys. Res.*, *103*(A4), 6693–6702, doi:10.1029/97JA03688.

Ku, H. C., and D. G. Sibeck (1998b), Flux transfer events produced by bursty merging at a single X line, *J. Geophys. Res.*, *103*(A7), 14,965–14,978, doi:10.1029/98JA01171.

Ku, H. C., and D. G. Sibeck (2000), Flux transfer events produced by the onset of merging at multiple X lines, *J. Geophys. Res.*, *105*(A2), 2657–2675, doi:10.1029/1999JA900431.

Lee, L. C., and Z. F. Fu (1985), A theory of magnetic flux transfer at the Earth's magnetopause, *Geophys. Res. Lett.*, *12*(2), 105–108, doi:10.1029/GL012i002p00105.

Lockwood, M., and M. A. Hapgood (1998), On the cause of a magnetospheric flux transfer event, *J. Geophys. Res.*, *103*(A11), 26,453–26,478, doi:10.1029/98JA02244.

Milan, S. E., M. Lester, S. W. H. Cowley, and M. Brittnacher (2000), Convection and auroral response to a southward turning of the IMF: Polar UVI, CUTLASS, and IMAGE signatures of transient magnetic flux transfer at the magnetopause, *J. Geophys. Res.*, *105*(A7), 15,741–15,755, doi:10.1029/2000JA900022.

Omidi, N., and D. G. Sibeck (2007), Flux transfer events in the cusp, *Geophys. Res. Lett.*, *34*, L04106, doi:10.1029/2006GL028698.

Raeder, J. (2006), Flux Transfer Events: 1. Generation mechanism for strong southward IMF, *Ann. Geophys.*, *24*(1), 381–392.

Roelof, E. C., and D. G. Sibeck (1993), Magnetopause shape as a bivariate function of interplanetary magnetic field Bz and solar wind dynamic pressure, *J. Geophys. Res.*, *98*(A12), 21,421–21,450, doi:10.1029/93JA02362.

Russell, C. T., and R. C. Elphic (1978), Initial ISEE magnetometer results: magnetopause observations, *Space Sci. Rev.*, *22*(6), 681–715, doi:10.1007/BF00212619.

Russell, C. T., and R. C. Elphic (1979), ISEE observations of flux transfer events at the dayside magnetopause, *Geophys. Res. Lett.*, *6*(1), 33–36, doi:10.1029/GL006i001p00033.

Sanny, J., C. Beck, and D. G. Sibeck (1998), A statistical study of the magnetic signatures of FTEs near the dayside magnetopause, *J. Geophys. Res.*, *103*(A3), 4683–4692, doi:10.1029/97JA03246.

Scholer, M. (1988), Magnetic flux transfer at the magnetopause based on single X line bursty reconnection, *Geophys. Res. Lett.*, *15*(4), 291–294, doi:10.1029/GL015i004p00291.

Scholer, M. (1989), Asymmetric time-dependent and stationary magnetic reconnection at the dayside magnetopause, *J. Geophys. Res.*, *94*(A11), 15,099–15,111, doi:10.1029/JA094iA11p15099.

Scholer, M. (1995), Models of flux transfer events, in *Physics of the magnetopause*, edited by P. Song, B. U. O. Sonnerup, and M. F. Thomsen, Geophysical Monograph, pp. 235–245, American Geophysical Union, Washington D. C.

Shue, J.-H., P. Song, C. T. Russell, J. T. Steinberg, J. K. Chao, G. Zastenker, O. L. Vaisberg, S. Kokubun, H. J. Singer, T. R. Detman, and H. Kawano (1998), Magnetopause location under extreme solar wind conditions, *J. Geophys. Res.*, *103*(A8), 17,691–17,700, doi:10.1029/98JA01103.

Sibeck, D. G. (1990), A model for the transient magnetospheric response to sudden solar wind dynamic pressure variations, *J. Geophys. Res.*, *95*(A4), 3755–3771, doi:10.1029/JA095iA04p03755.

Sibeck, D. G. (1992), Transient events in the outer magnetosphere: Boundary waves or flux transfer events?, *J. Geophys. Res.*, *97*(A4), 4009–4026, doi:10.1029/91JA03017.

Sibeck, D. G., M. Kuznetsova, V. Angelopoulos, K.-H. Glaß meier, and J. P. McFadden (2008), Crater FTEs: Simulation results and THEMIS observations, *Geophys. Res. Lett.*, *35*, L17S06, doi:10.1029/2008GL033568.

Southwood, D. J., C. J. Farrugia, and M. A. Saunders (1988), What are flux transfer events?, *Planet. Space Sci.*, *36*(5), 503–508, doi:10.1016/0032-0633(88)90109-2.

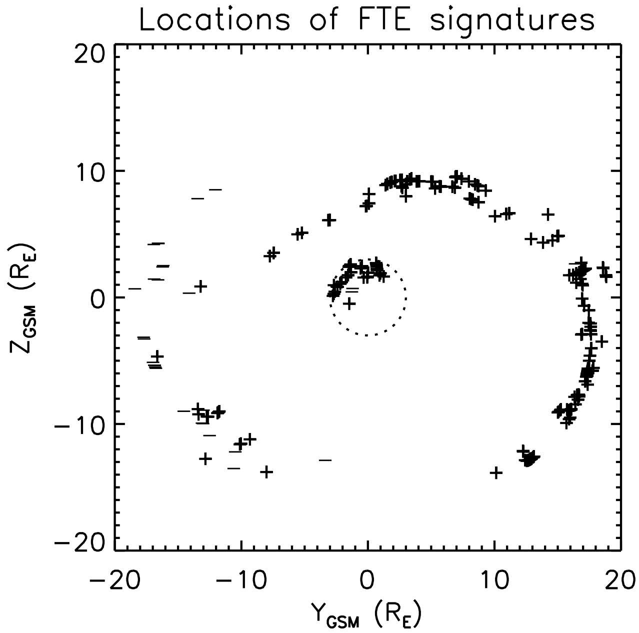

Figure 1: The location of each flux transfer event signature used in this study, projected into the GSM Y-Z plane. The dotted circle delineates the subsolar region $[(Y^2_{GSM} + Z^2_{GSM})^{\frac{1}{2}} < 3\ R_E]$. The flux transfer events outside the subsolar region are events catalogued by *Fear et al.* (2005), all of which were observed by all four Cluster spacecraft between November 2002 and June 2003. The events within the subsolar region were observed by one or more Cluster spacecraft in March 2007 and March/April 2008. A standard (+) or reverse (-) polarity signature is indicated by the plotting symbol.

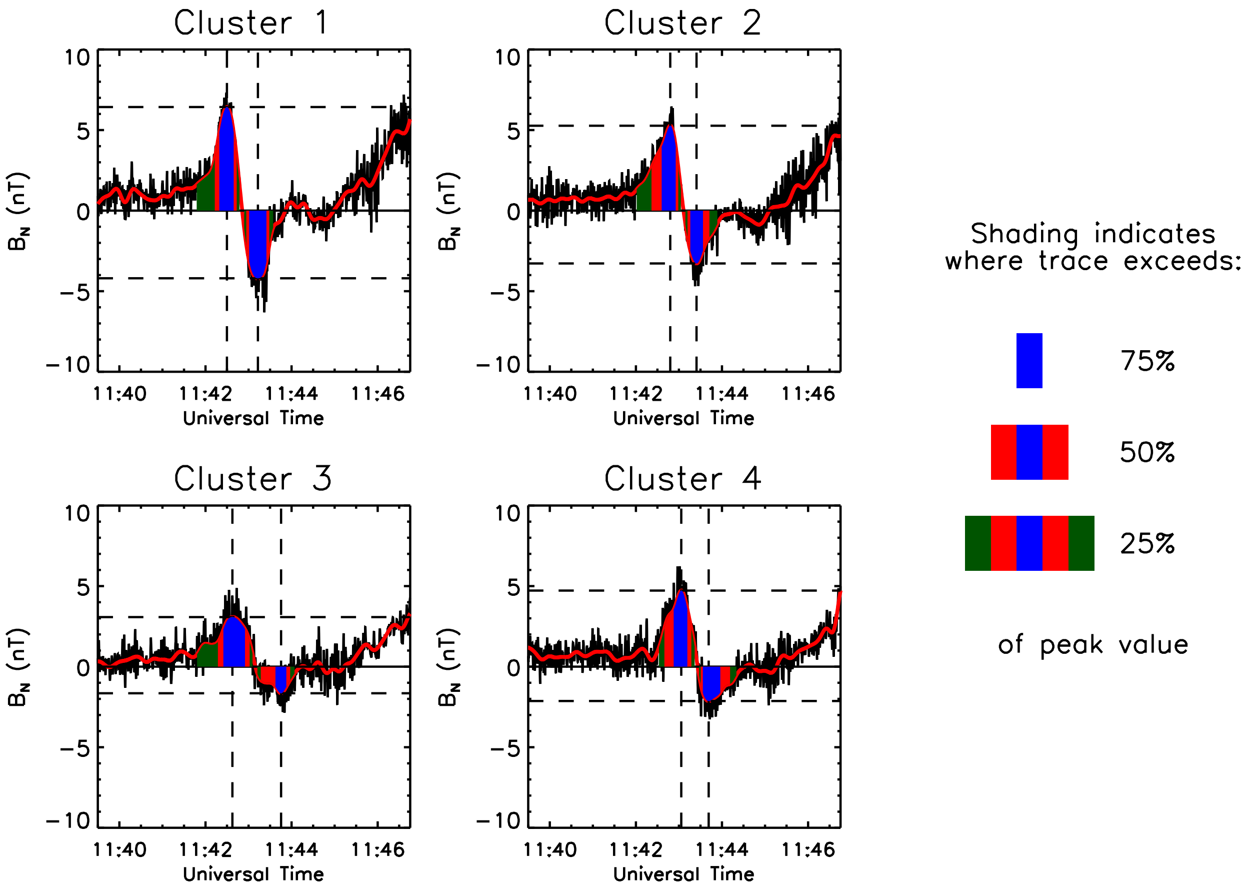

Figure 2: The B_N traces observed by the four Cluster spacecraft for an example FTE (10th November 2002, 11:43 UT). Each panel shows the observed B_N trace (black), overplotted with the filtered B_N trace (red). Guidelines identifying the values and times of the peak amplitudes for the leading and trailing peaks are shown by dashed lines. The areas under the B_N traces, where the traces exceed the quarter-/half-/three-quarter-maximum values, are shaded in green, red and blue.

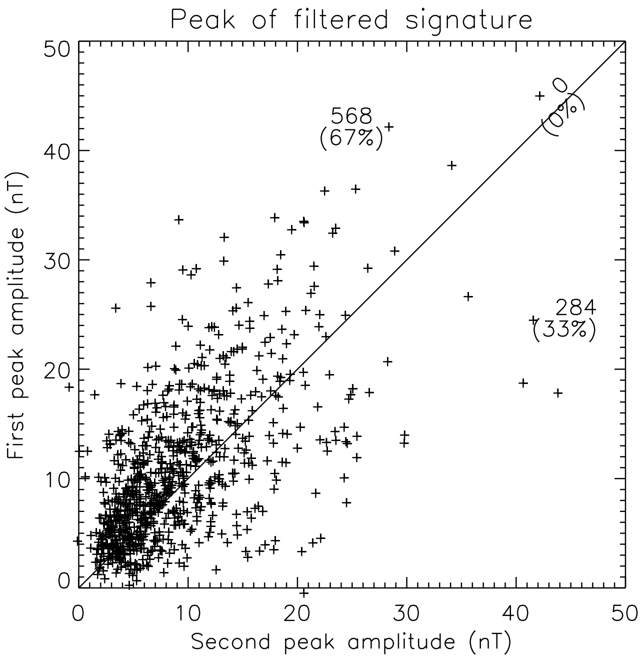

Figure 3: The amplitude of the leading peak plotted against the amplitude of the trailing peak for each filtered B_N trace observed by Cluster at high latitudes or on the flank (Section 2.1). The numbers represent the total number (and percentage) of traces where the amplitude of the leading peak is greater than, equal to, and less than the amplitude of the trailing peak.

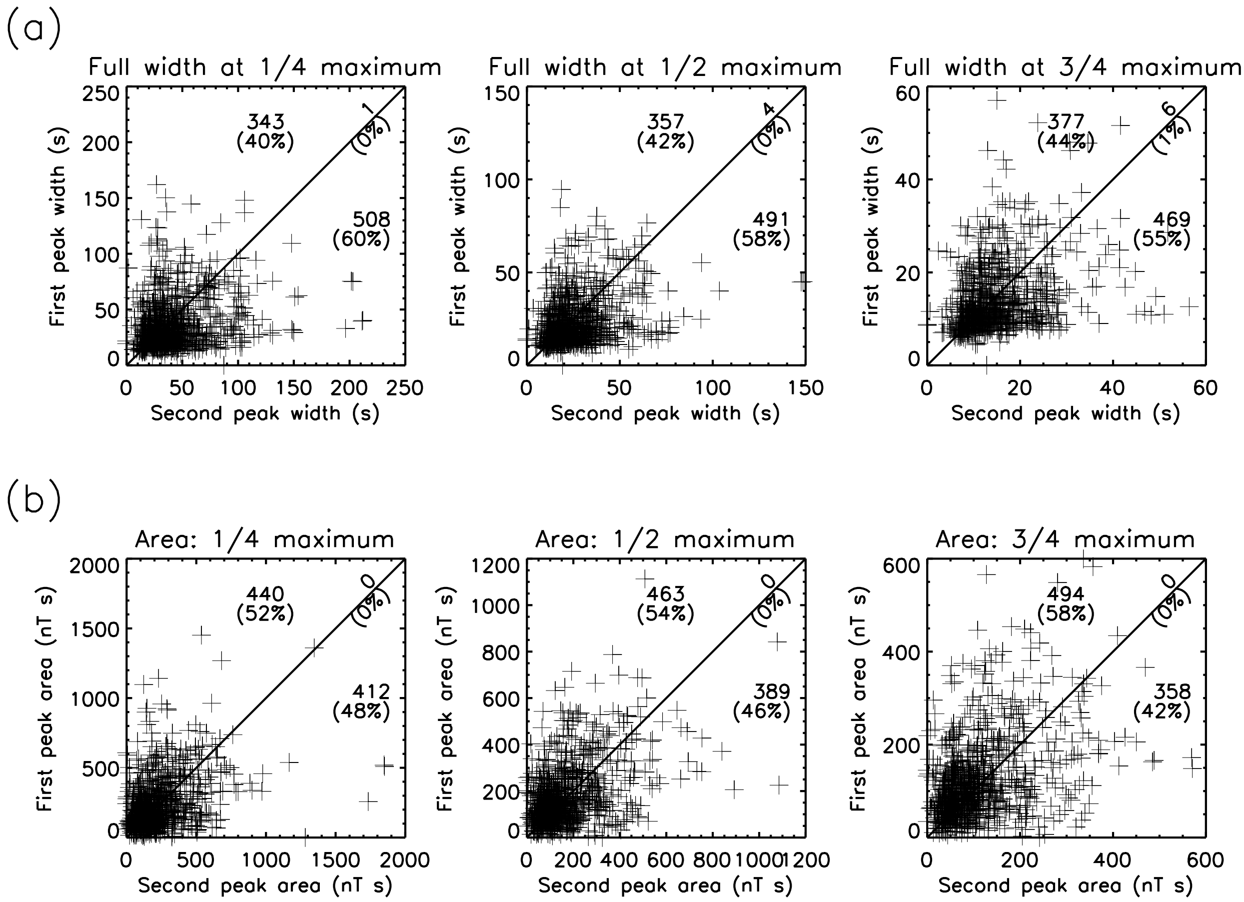

Figure 4: For the flux transfer event signatures observed at high latitudes and on the flanks (Section 2.1): (a) The widths of the filtered B_N trace peaks at 25%, 50% and 75% of the peak value, and (b) the areas under the trace and between each threshold. Each panel takes the same format as Figure 3.

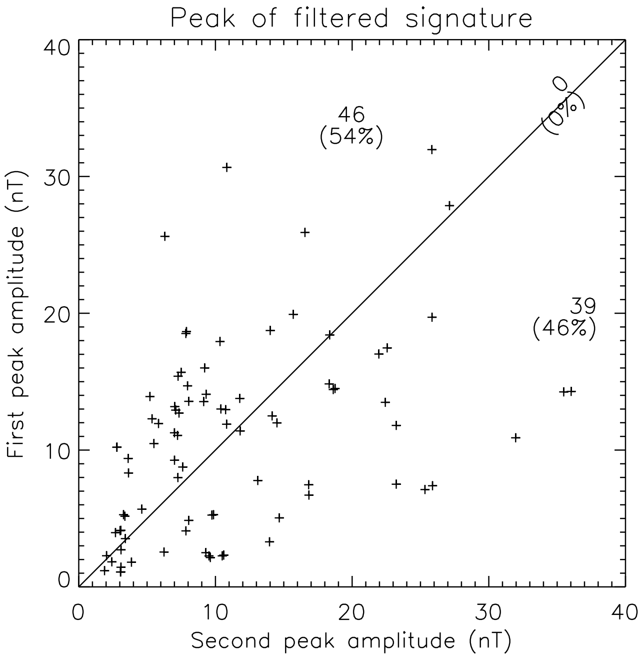

Figure 5: The amplitude of the leading peak plotted against the amplitude of the trailing peak for each filtered B_N trace observed by Cluster in the subsolar region (Section 2.2). The format of the figure is the same as Figure 3.

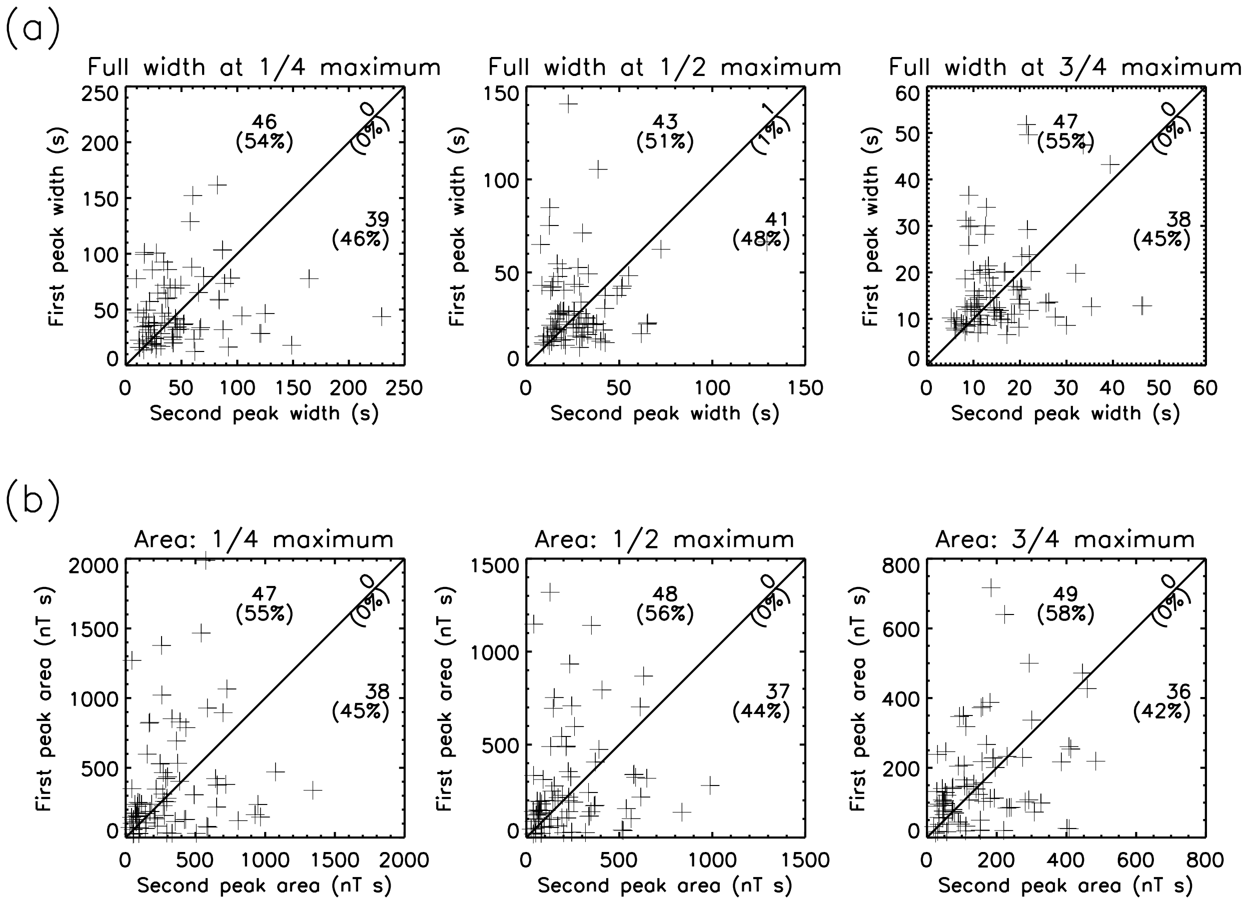

Figure 6: For the flux transfer event signatures observed in the subsolar region (Section 2.2): (a) The widths of the filtered B_N trace peaks at 25%, 50% and 75% of the peak value, and (b) the areas under the trace and between each threshold. Each panel takes the same format as Figure 3.

Table 1: The leading/trailing peak amplitude, widths and areas of the example FTE signatures in Figure 2. Amplitude/width/area 1 refers to the leading peak, and amplitude/width/area 2 refers to the trailing peak. The widths and areas are measured at 25% of the peak amplitude. In the notation used by *Sanny et al.* (1998), α and β refer to the amplitudes of the leading and trailing peaks respectively.

Spacecraft	Amplitude 1 (α) [nT]	Amplitude 2 (β) [nT]	α/β	Width 1 [s]	Width 2 [s]	Area 1 [nT s]	Area 2 [nT s]
Cluster 1	6.43	4.20	1.53	59.6	40.4	224	128
Cluster 2	5.27	3.28	1.61	61.6	44.4	198	97
Cluster 3	3.08	1.65	1.86	77.2	51.8	155	56
Cluster 4	4.72	2.13	2.21	49.8	52.0	159	78

Table 2: A comparison of the asymmetry observed at high latitudes/on the flank in the present study (Section 2.1), in the subsolar region in the present study (Section 2.2), and in the subsolar region in the *Sanny et al.* (1998) study. Events are split according to a classification based on that used by *Sanny et al.*. The amplitudes of the leading and trailing peaks are denoted by α and β respectively. The figures in parentheses indicate the total number of B_N traces in each category. The bottom row shows the distribution of asymmetry in the subsolar observations in the present study, if the same selection criteria as used by *Sanny et al.* are applied (i.e. if all traces with a peak-to-peak B_N amplitude less than 5 nT or duration less than 1 minute are excluded).

	$\alpha > 1.25\beta$	$1.25\beta > \alpha > 0.75\beta$	$0.75\beta > \alpha$
High lat./flank	49% (417)	31% (261)	20% (174)
Subsolar	41% (35)	26% (22)	33% (28)
Sanny et al.	0	72% (79)	28% (31)
Subsolar (Same criteria as *Sanny et al.*)	41% (26)	27% (17)	33% (21)